AGRICULTURE AND NATURAL RESOURCES

Journal homepage: http://anres.kasetsart.org

Research article

Optimizing prediction of key water quality parameters in tilapia river-based cage culture system using simple parameters based on different deep learning models

Roongparit Jongjaraunsuk, Wara Taparhudee*

Department of Aquaculture, Faculty of Fisheries, Kasetsart University, Bangkok 10900, Thailand

Article Info

Article history:
Received 14 September 2024
Revised 11 June 2025
Accepted 3 July 2025
Available online 31 July 2025

Keywords:
Convolutional neural network (CNN),
Deep learning (DL),
Hybrid CNN-LSTM,
Long short-term memory (LSTM),
Water quality

Abstract

Importance of the work: Deep learning (DL) models can predict key water quality values in red tilapia culture using easily measured parameters.

Objectives: To enhance the efficiency and effectiveness of water quality monitoring by developing a predictive DL model.

Materials and Methods: Convolutional neural network (CNN), long short–term memory (LSTM) and a hybrid CNN–LSTM model were fine–tuned using the Python software. Model performance was assessed using root mean square error (RMSE), mean absolute error (MAE), normalized root mean square error (NRMSE), Nash–Sutcliffe efficiency (NSE) and the coefficient of determination (R^2). The results were statistically analyzed based on a t test.

Results: During data collection, the mean ± SD values of water quality parameters were: dissolved oxygen (DO), 4.03 ± 0.41 mg/L; water temperature (Temp), 27.63 ± 1.42°C; water pH level (pH), 7.45 ± 0.11; total ammonia nitrogen (TAN) at 0.14 ± 0.04 mg/L; nitrite–nitrogen (NO_2^-–N), 0.04 ± 0.05 mg/L; alkalinity (ALK), 105.41 ± 9.94 mg/L; and water transparency (Trans), 75.31 ± 22.80 cm. The study evaluated the CNN, LSTM and CNN–LSTM models, with CNN–LSTM consistently offering the best balance of accuracy and processing speed. Specifically, it excelled at 1,000 epochs for DO and TAN predictions and at 2,000 epochs for NO_2^-–N and ALK predictions, with no significant differences compared to observed values using standard measurement methods.

Main finding: The hybrid CNN–LSTM model that used easily measurable water quality parameters (Temp, pH and Trans), effectively predicted more difficult–to–measure water quality parameters (DO, TAN, NO_2^-–N and ALK). Additionally, the hybrid model outperformed the individual CNN and LSTM models, providing better prediction accuracy and faster processing times.

* Corresponding author.
E-mail address: ffiswrt@ku.ac.th (W. Taparhudee)

https://doi.org/10.34044/j.anres.2025.59.4.12

Introduction

Aquaculture plays important roles in food security and economic growth, especially in developing countries. For example, tilapia farming systems have been developed in ponds and cages, with cage farming in rivers being particularly widely practiced due to its high yield and good quality (FAO, 2020). Appropriate water quality is crucial for the success of these culture systems, as it directly affects the health and growth of the fish. Water quality parameters, such as dissolved oxygen (DO), total ammonia nitrogen (TAN), nitrite–nitrogen (NO_2^-–N) and alkalinity (ALK), are important for fish culture (Boyd and Tucker, 2012). Measuring these parameters can be labor–intensive, time–consuming, require expensive equipment and some of them must be done in the laboratory by an expert, whereas other parameters, such as water temperature (Temp), water pH level (pH) and water transparency (Trans), are also important; however, their measurement is easier since it requires inexpensive equipment and can be done more frequently. Therefore, the purpose of the current research was to develop a predictive model utilizing easily measurable parameters, such as Temp, pH and Trans, to predict important water quality indicators, namely DO, TAN, NO_2^-–N and ALK, in a red tilapia river–based cage culture system.

In recent years, the utilization of machine learning (ML) and deep learning (DL) has notably increased as a pivotal technique in data analysis for many purposes. For example, there have been many application of these techniques in water quality prediction, such as reported by Palani et al. (2008), who utilized artificial neural networks (ANNs) to predict and forecast water quality based on salinity, Temp, DO and chlorophyll–a in Singapore's coastal waters. In addition, Liu et al. (2019) developed a drinking–water quality prediction model using long short–term memory (LSTM) deep neural networks to handle a complex large dataset generated by IoT–based monitoring systems. Ahmed et al. (2019) reported the use of gradient boosting and polynomial regression as the most effective for water quality index (WQI) prediction, while multi–layer perceptron (MLP) was applied to efficiently predict WQI. Castrillo and López García (2020) demonstrated the high accuracy of using random forest (RF) compared to linear models to estimate nutrient concentrations based on commonly measured in–situ water quality surrogates. Zambrano et al. (2021) applied RF to forecast key variables, such as DO and pH, even with minimal data, offering practical solutions for fish farmers using affordable mobile technology. Li et al. (2022) demonstrated that support vector machine (SVM) provided the most accurate and stable predictions for water quality parameters in industrial aquaculture systems. Ye et al. (2022) utilized absorbance data across all ultraviolet–visible light wavelengths and convolutional neural networks (CNNs) to predict chemical oxygen demand. Anand et al. (2023) developed a water quality prediction model using CNN to assess water suitability based on color and quality parameters, utilizing image processing to make predictions from mobile and satellite images. Wang et al. (2023) also demonstrated that LSTM and SVM effectively predicted water quality parameters. with their models using four key parameters: Temp, turbidity, pH and total dissolved solids.

In addition, combinations of various models have been applied to obtain more accurate results. For example, Chen et al. (2021) demonstrated that the LSTM network achieved high accuracy and F1–scores, while the genetic algorithm-optimized SVM model was the most effective for variable-flow regulation. Juna et al. (2022) developed a nine–layer MLP combined with a K–nearest neighbor (KNN) imputer to address missing data and enhance water quality prediction accuracy. Chen et al. (2022) used LSTM networks enhanced with an attention mechanism (AT–LSTM) to forecast DO levels in the Burnett River, Australia. Wu and Wang (2022) developed a hybrid model combining ANNs, discrete wavelet transform and LSTM for predicting water quality in the Jinjiang River. Zhou et al. (2022) introduced a hybrid prediction framework combining wavelet decomposition, autoregressive integrated moving average (ARIMA) and gated recurrent unit (GRU) models, named wavelet decomposition (W)-ARIMA–GRU, to enhance water quality prediction accuracy. Cai et al. (2023) introduced a Kalman filter–enhanced LSTM (KF–LSTM) encoder–decoder network to address water quality prediction challenges with missing data. Yang et al. (2023) developed a hybrid DL framework for water quality prediction in recirculating aquaculture system (RAS), integrating CNN, GRU and an Attention mechanism. Jongjaraunsuk et al. (2024) found that the CNN–LSTM model at 5,000 epochs achieved high prediction accuracy for most parameters, except pH, highlighting its effectiveness in optimizing water quality management in aquaculture systems.

Based on the promising results from these studies, the current research applied advanced DL techniques (specifically CNN, LSTM networks and hybrid CNN–LSTM models) to predict the key water quality parameters mentioned earlier. LSTMs excel at remembering information over long periods (Chen et al., 2021), which can be beneficial despite the

potential impact of older data on model accuracy. CNNs could automatically detect important features without human supervision (Alzubaidi et al., 2021), while the hybrid CNN–LSTM model combined the strengths of both approaches, potentially offering superior prediction performance (Pan et al., 2023; Jongjaraunsuk et al., 2024).

In summary, the current research aimed to enhance the efficiency and effectiveness of water quality monitoring in red tilapia river-based aquaculture systems by developing a predictive model using easily measurable water quality parameters to predict important but difficult–to–measure water quality parameters, to inform appropriate water quality management. A successful outcome should help to promote the productivity and sustainability of the aquaculture system.

Materials and Methods

Ethical statement

The study adhered to applicable guidelines and regulations, conducting all methods with approval (ACKU 67–FIS–018) from the Kasetsart University Institutional Animal Care and Use Committee, Bangkok, Thailand. However, this research did not involve the use of animals in any way as only water quality samples were collected and measured during the experiment.

Study area and data collection

The Fish Bear Farm is located in Tha Muang district, Kanchanaburi province, Thailand (13°58'15"N 99°34'46"E). The farm raises red tilapia in the Mae Klong River area (Fig. 1). The farm consists of 232 fish cages, each measuring 5 m × 5 m × 2.5 m (width × length × depth). These are divided into 59 cages (25%) for raising small fish, 169 cages (73%) for raising large fish and 4 unused cages (2%), as shown in Fig 2. The cages for raising small fish start with fish fry averaging 1.5 g each and grow them to about 20 g over approximately 1 mth. Then, the fish are transferred to the cages for raising until larger (mean size of 800–1,000 g per fish) over approximately 4–6 mth. The stocking density in both the small and large fish cages was 1,500 fish per cage (24 fish/m^3).

Data collection was conducted in eight large fish cages over two culture cycles (Fig. 2). Water quality was measured and recorded before feeding in the morning (0700–0800 hours) and in the late afternoon (1600–1700 hours) on each sampling day. During the culturing period, the fish were fed a diet containing 30% protein (SPM 042R; S.P.M. Feedmill Co., Ltd; Ratchaburi, Thailand) three times a day. Feeding was done by hand and continued until the fish were satiated.

Water quality measurement

In total, 4,032 (18 wk × 8 cages × 2 times a day × 7 parameters × 2 culturing crops) water samples were analyzed for various parameters (DO, Temp, pH, TAN, NO_2^-–N, ALK and Trans). DO and Temp were measured using a YSI Pro20i instrument (YSI; Yellow Springs, OH, USA), while pH levels were determined using a YSI pH100A instrument (YSI; Yellow Springs, OH, USA). Trans was assessed using a Secchi disc with a two–color design. The concentrations of ALK, TAN and NO_2^-–N were determined in the laboratory, adhering to the protocols established by the American Public Health Association (2005).

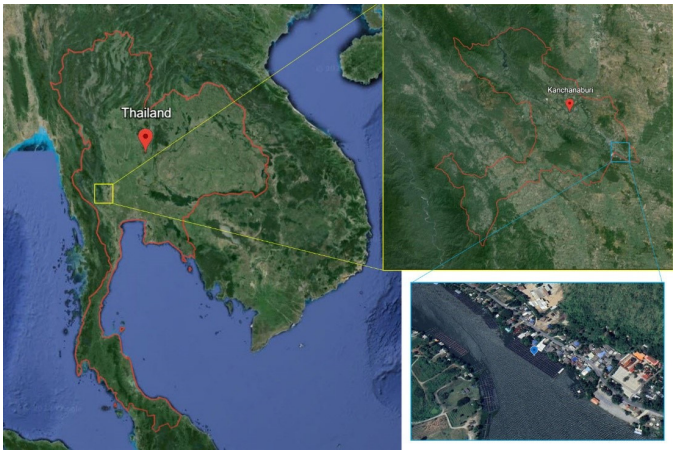

Fig. 1 Location overview of study area, showing location of Kanchanaburi province in Thailand, focusing on specific study site along the riverbank (see insets), where smaller satellite image provides closer view of area of interest, showing more detailed geographical features and nearby structures

Fig. 2 Layout of 232 cages in experimental farm, consisting of 59 cages for rearing small fish (bound by yellow line) and 169 cages for rearing large fish (bound by red line), with large fish cages, numbered 1–8, specifically used for data collection

Feature selection

This research aimed to improve the predictive model by utilizing easily measurable parameters (Temp, pH and Trans) to predict key water quality indicators, namely DO, TAN, NO_2^-–N, ALK in a red tilapia cage–river–based culture system.

Jongjaraunsuk et al. (2024) identified substantial correlations among these water quality indicators in red tilapia aquaculture within an outdoor recirculation system using DL and hybrid modeling approaches. Their findings highlighted Temp as the most influential factor for DO, as higher Temp reduced oxygen solubility. Trans played a crucial role in predicting TAN and ALK due to its association with organic matter and suspended particles. Additionally, ALK was a dominant predictor for NO_2^-–N, as it influenced nitrogen cycle dynamics. However, pH had weaker predictive power for these parameters, likely due to its dependence on unmeasured environmental factors such as CO_2 levels and biological activity. These findings underscored the importance of Temp and Trans in water quality modeling, with the CNN–LSTM hybrid model effectively capturing these nonlinear relationships for DO, TAN, NO_2^-–N and ALK.

While RF was effectively used to identify key parameter correlations, certain limitations remain. Parameters such as ALK, TAN and NO_2^-–N are not easily measurable in real–time under typical aquaculture conditions, as they require laboratory analysis, making them impractical for continuous monitoring. To address this challenge, the current study focused on more readily available parameters (Temp, Trans and pH) since these can be monitored in real–time. Although Jongjaraunsuk et al. (2024) found that pH had a weaker correlation with other parameters, it was included in the current study due to its known, albeit limited, influence on water quality dynamics. This approach help to ensure that the predictive model would remain feasible for real–world applications, even if it required a trade–off in accuracy due to the exclusion of parameters that are harder to measure continuously.

Convolutional neural networks

A CNN is a type of supervised neural network, with a basic structure consisting of an input layer, convolutional layers, pooling layers (also know as subsampling layers), fully connected layers and an output layer. A typical CNN includes multiple convolutional layers; although pooling layers are not strictly necessary, they are commonly included after convolutional layers in CNN architectures (You et al. 2020). The basic CNN structure is illustrated in Fig. 3A

Long short-term memory

LSTM is a memory–enabled ANN that is suitable for processing and predicting important events that involve time (Lin et al. 2021). LSTM is developed from the recurrent neural network model, with the working principle that it can store the "state" or information of each node. This allows it to trace and understand the origin of the data, knowing what the original value was. The LSTM technique has a special function that acts as a "gate" that controls the data that comes into each node, consisting of forget gate layers, an input gate layer and an output gate layer (Jiang et al. 2019), as shown in Fig. 3B, for which the working steps are:

1) The forget gate layer is a gate that is responsible for determining whether the data entering the cell state should be kept or discarded. Data that are kept are evaluated by the input data that enters that node together with the result of the calculation of the previous node, based on the sigmoidal function, as shown in Equation 1:

$$f_t = \sigma\left(W_f \cdot [h_{t-1}, x_t] + b_f\right) \quad (1)$$

where f_t is the forget gate (value between 0 and 1), σ is the sigmoid function, W_f is the weight of the matrices, h_{t-1} is the output value of the previous cell state, x_t is the input value into the cell state at time t and b_f is the bias value.

2) The input gate layer or gate is used to receive new input data and then to record or write the data to each node. The operation is divided into 2 parts: i) checking the update cell state when receiving input data based in the sigmoidal function, which controls the input gate in choosing whether or not to use the update cell state; and ii) if the updated cell state is chosen, the tanh function creates candidate values ($\widetilde{C}_t$) in the state, as shown in Equations 2 and 3:

$$i_t = \sigma\left(W_i \cdot [h_{t-1,} x_t] + b_i\right) \quad (2)$$

$$\widetilde{C}_t = \tanh\left(W_c \cdot [h_{t-1,} x_t] + b_C\right) \quad (3)$$

where the subscript *i* represent the process in the input gate layer.

3) The output gate layer prepares data to be output based on examining the cell state that has already undergone various calculation processes. The sigmoidal function is applied to choose which data in the cell state will be output. Then, the cell state value is used in the tanh function (where the obtained value is 1 or -1); subsequently, the value obtained

from the tanh function is used with the output value obtained from the sigmoid gate to calculate the output value, based on Equation 4:

$$O_t = \sigma\,(W_0 \cdot [h_{t\text{-}1}, x_t] + b_0) \quad (4)$$

where subscript o represent the process in the output gate layer, O_t is the output gate, σ is the sigmoidal function, W_0 is the weight of the matrices, $h_{t\text{-}1}$ is the output value of the previous cell state (at time stamp t-1), x_t is the input value coming into the cell state at time t, b_0 is the bias value.

Convolutional neural network–long short–term memory

The proposed general CNN–LSTM architecture is presented in Fig. 3C.

The current study implemented a CNN–LSTM hybrid model to analyze the time-series data. The architecture commenced with a 1D convolutional layer, consisting of 1,024 filters and a kernel size of 3, which applied the ReLU activation function. This layer was designed to capture local patterns in the input data, with the input shape defined as "(X_train.shape[1], 1)", indicating that the model expects one–dimensional data with a length equal to the number of time steps in the training set. Following the convolutional layer, a max–pooling layer with a pool size of 1 was used to downsample the feature maps, potentially preserving the temporal structure while reducing dimensionality. The structures of our CNN–LSTM developed models contained the following details:

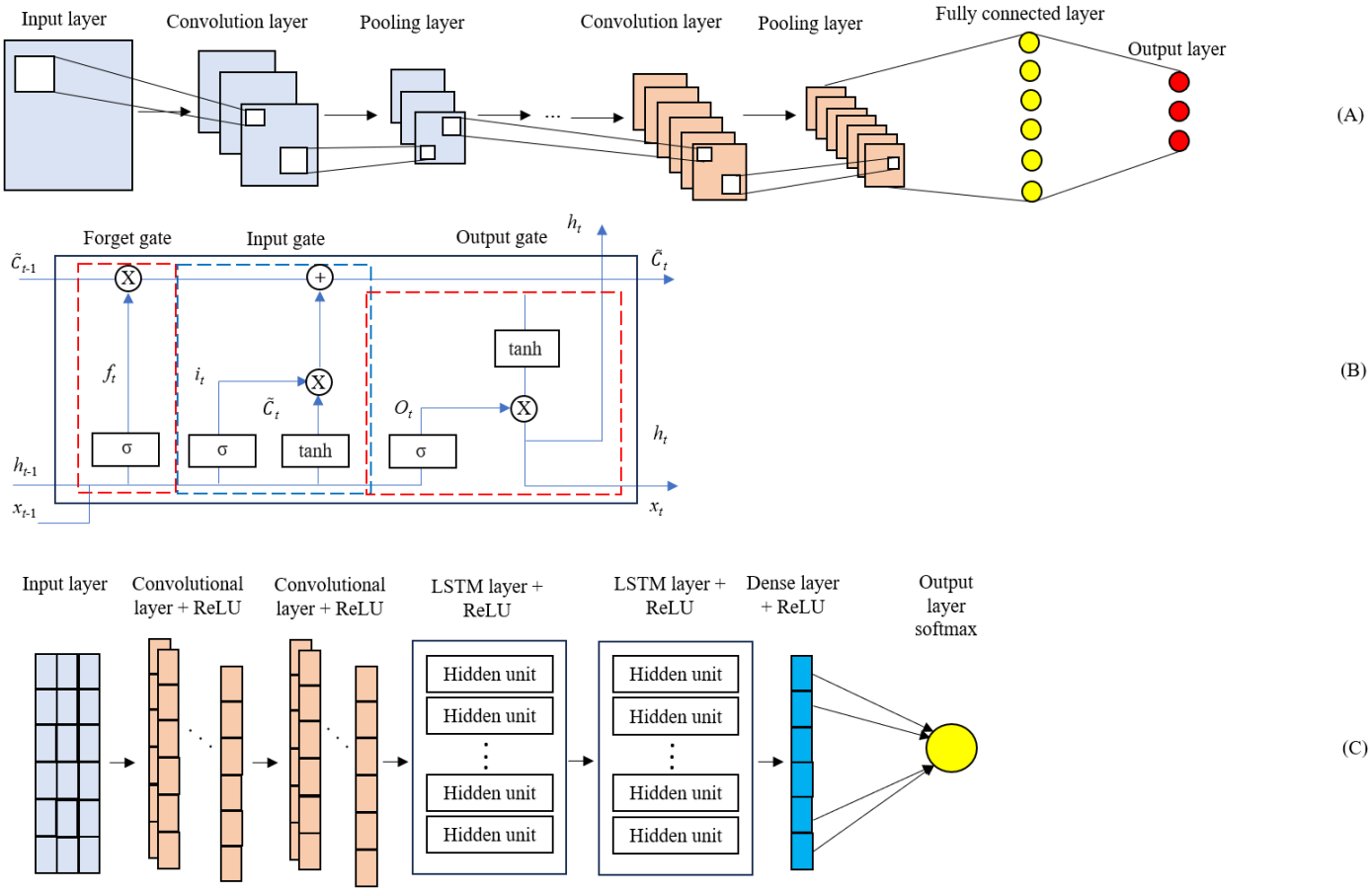

Fig. 3 (A) Convolutional neural network (CNN) architecture, showing CNN with input layer and convolutional and pooling layers for feature extraction and dimensionality reduction, respectively, followed by fully connected and output layers for final classification; (B) long short–term memory (LSTM) cell structure, detailing components of LSTM cell, including forget, input and output gates, where these gates regulate flow and transformation of information, allowing cell to maintain long–term dependencies in sequential data; (C) Hybrid CNN–LSTM, showing integration of CNN and LSTM components, starting with convolutional layers for spatial feature extraction and transitioning to LSTM layers for capturing temporal dependencies, with dense layer and SoftMax output layer finalizing the model for classification tasks. The Rectified linear unit (ReLU) activation function is applied in various layers to introduce non–linearity and improve learning performance

```
Model = sequential (),
Model.add (conv1D(1024. Kernel_size = 3, activation = 'relu',
Input_shape = (X_train.shape [1], 1)))
Model.add (maxpooling1D (pool_size = 1))
Model.add (LSTM (300, return_sequences = True))
Model.add (LSTM (300))
Model.add (dense (128, activation = 'relu'))
Model.add (dropout (0.5))
Model.add (dense(1, activation = 'linear'))
Model.compile (optimizer = 'adam', loss = 'mean_squared_
error', metrics = ['mae'])
```

Data processing, analysis and visualization

Python (version 3.9; Python software foundation, executed within the google colaboratory cloud–based notebook environment), was used for essential tasks encompassing DL and data analysis. Data processing utilized the Python library (pandas) for data manipulation, while scikit–learn was used for dataset splitting and feature scaling (Min–Max Scaler) and TensorFlow was used for handling neural network models, such as Sequential, Conv1D, MaxPooling1D, LSTM, Dense, Flatten and Dropout, alongside importing evaluation metrics: root mean square error (RMSE), mean absolute error (MAE), normalized root mean square error (NRMSE), Nash–Sutcliffe efficiency (NSE) and the coefficient of determination (R^2) from scikit–learn to assess model performance. Matplotlib (version 3.8; Matplotlib development team) was used for data visualization, enabling the creation of graphs, charts and other visual representations of the data and model outputs within the Colab notebook.

The process began with data preparation. The data were loaded and divided into two datasets: 80% for training and 20% for testing. Then, three models (CNN, LSTM and hybrid CNN–LSTM) were used in prediction analysis. An iterative fine–tuning approach was implemented to optimize each model's performance, starting with 1,000 epochs and increasing the count by 500 in each step. This process continued until a decrease in accuracy was observed. For clarity, an epoch represented a complete pass of the training data through the model during the learning phase.

Performance metrics and data analysis

The performance of each model was assessed using RMSE, MAE, NRMSE, NSE and R^2. These metrics were, calculated using Equations 5–9, respectively:

$$RMSE = \sqrt{\frac{\Sigma_{i=1}^{N} (y_{measured.i} - y_{predict.i})^2}{N}} \quad (5)$$

$$MAE = \frac{\Sigma_{i=1}^{N} |y_{measured.i} - y_{predict.i}|}{N} \quad (6)$$

$$NRMSE = \sqrt{\frac{\Sigma_{i=1}^{N} (y_{measured.i} - y_{predict.i})^2}{y_{max} - y_{min}}} \quad (7)$$

where $y_{measured}$ is the observed value, $y_{predict}$ is the predicted value, N is the total number of variables, y_{max} is the maximum value and y_{min} is the minimum value.

$$NSE = 1 - \frac{\Sigma_{i=1}^{N} (Obs_t - Sim_t)^2}{\Sigma_{i=1}^{N} (Obs_t - \overline{Obs})^2} \quad (8)$$

where Obs_t is the observed value at time t, Sim_t is the simulated (predicted) value at time t and $\overline{Obs}$ is the mean of the observed values:

$$R^2 = 1 - \frac{SS_{res}}{SS_{tot}} \quad (9)$$

where: SS_{res} is the sum of squares of residuals (also known as the sum of squared errors), representing the difference between the predicted values and the actual values, and SS_{tot} is the total sum of squares, measuring the total variance of the dependent variable (the target) from its mean. In addition, the calculation time for each model was measured.

The results from using the simple parameters (pH, Temp and Trans) to predict difficult ones (DO, TAN, NO_2^-–N and ALK) were compared with the actual values, based on the self–test method. Statistical analysis was performed to compare the mean differences using an independent sample t test at the 95% confidence level, employing IBM SPSS Statistics version 26 (IBM Corp., Armonk, NY, USA). Data were presented as mean ± SD.

Results

Water quality

Throughout the data collection period, the mean DO value was 4.03 ± 0.41 mg/L, with a range of 3.36–4.77 mg/L. The mean Temp value was 27.63 ± 1.42°C, with a range of 25.20–30.50°C. The mean pH value was 7.45 ± 0.11, with a range of 7.11–7.60, the mean TAN value was 0.14 ± 0.04 mg/L, with a range of 0.09–0.22 mg/L, while the mean NO_2^-–N value was 0.04 ± 0.05 mg/L, with a range of 0.00–0.14 mg/L.

The mean ALK value was 105.41 ± 9.94 mg/L, with a range of 92.00–125.00 mg/L and the mean Trans value was 75.31 ± 22.80 cm, with a range of 19.00–110.00 cm, as shown in Table 1.

Prediction performance

The comparative results of the prediction performance using the values for RMSE, MAE, NRMSE, NSE, R^2 and different processing times for the CNN, LSTM and CNN–LSTM models are shown in Table 2. After fine–tuning the different groups of models, based on the results for predicting DO values, the CNN model had the best prediction results (least error) at 3,500 epochs, LSTM at 3,500 epochs and CNN–LSTM at 1,000 epochs, with mean RMSE values of 0.345, 0.372 and 0.370, respectively, and no significant differences for all three models between the mean prediction value and the actual measured value. However, based on processing time, the CNN–LSTM model with 1,000 epochs was significantly ($p < 0.01$) the fastest model at 86 s, followed by the CNN model with 3,500 epochs at 168 s and the LSTM model with 3,500 epochs at 264 s, respectively.

Table 1 Mean ± SD values and minimum and maximum values, with optimal ranges for water quality parameters for fish growth.

Parameter	Unit	Value (range)	Optimal value	Reference
DO	mg/L	4.03 ± 0.41 (3.36–4.77)	>3	Kolding et al. (2008); Tran-Duy et al. (2012)
Temp	°C	27.63 ± 1.42 (25.20–30.50)	25–32	Azaza et al. (2008)
pH		7.45 ± 0.11 (7.11–7.60)	7–8	Lawson, (1995); El-Sherif and El-Feky, (2009)
TAN	mg/L	0.14 ± 0.04 (0.09–0.22)	<0.5	Hargreaves and Tucker, (2004)
NO_2^-–N	mg/L	0.04 ± 0.05 (0.00–0.14)	<0.5	Lawson, (1995); Stone and Thomforde, (2004)
ALK	mg/L	105.41 ± 9.94 (92.00–125.00)	75–400	Lawson, (1995), Boyd and Tucker, (2012)
Trans	cm	75.31 ± 22.80 (19.00–110.00)	19.6–100*	Taparhudee et al. (2024)

DO = dissolved oxygen; Temp = water temperature; pH = water pH level; TAN = total ammonia nitrogen; NO_2^-–N = nitrite–nitrogen; ALK = alkalinity; Trans = water transparency.

* Raising tilapia in cages, especially in river cages, within Trans range of 19.6–100.0, had no effect on the fish throughout the culture period, according to Taparhudee et al. (2024).

Table 2 Comparison of performance metrics and processing times for three different models (convolutional neural network (CNN), long short-term memory (LSTM) and a hybrid CNN–LSTM model) and optimal epoch setting, where gray shading and bold in cells shows best-optimized prediction model for each water quality parameter.

Parameter	Model tuning (epoch)	RMSE	MAE	NRMSE	NSE	R^2	Processing time (s)
DO	CNN 1,000	0.383	0.323	0.272	0.104	0.104	40
	CNN 1,500	0.373	0.316	0.265	0.148	0.148	68
	CNN 2,000	0.367	0.303	0.261	0.177	0.177	120
	CNN 2,500	0.358	0.298	0.255	0.215	0.215	129
	CNN 3,000	0.353	0.286	0.251	0.236	0.236	144
	CNN 3,500	**0.345**	**0.264**	**0.245**	**0.271**	**0.271**	**168**
	CNN 4,000	0.373	0.269	0.265	0.149	0.149	181
	CNN 4,500	0.413	0.272	0.294	-0.044	-0.044	197
	LSTM 1,000	0.400	0.347	0.283	0.033	0.333	148
	LSTM 1,500	0.400	0.347	0.280	0.037	0.037	168
	LSTM 2,000	0.398	0.340	0.283	0.033	0.033	204
	LSTM 2,500	0.390	0.330	0.278	0.066	0.066	220
	LSTM 3,000	0.382	0.320	0.272	0.106	0.106	227
	LSTM 3,500	**0.372**	**0.312**	**0.266**	**0.144**	**0.144**	**264**
	LSTM 4,000	0.386	0.320	0.274	0.084	0.084	328
	LSTM 4,500	0.433	0.300	0.306	0.093	0.093	389
	CNN–LSTM 1,000	**0.370**	**0.307**	**0.263**	**0.164**	**0.164**	**86**
	CNN–LSTM 1,500	0.373	0.299	0.265	0.150	0.150	133
	CNN–LSTM 2,000	0.513	0.359	0.365	-0.641	-0.641	195
TAN	CNN 1,000	0.027	0.019	0.201	0.581	0.581	59
	CNN 1,500	**0.027**	**0.018**	**0.200**	**0.584**	**0.584**	**83**
	CNN 2,000	0.028	0.017	0.209	0.544	0.544	120
	CNN 2,500	0.030	0.017	0.221	0.491	0.491	148
	LSTM 1,000	0.036	0.030	0.262	0.282	0.282	149
	LSTM 1,500	0.035	0.030	0.255	0.310	0.310	152
	LSTM 2,000	**0.030**	**0.020**	**0.244**	**0.370**	**0.370**	**187**
	LSTM 2,500	0.034	0.026	0.258	0.292	0.292	204

Table 2 Coutinued

Parameter	Model tuning (epoch)	RMSE	MAE	NRMSE	NSE	R^2	Processing time (s)
	LSTM 3,000	0.038	0.026	0.300	0.166	0.166	258
	CNN–LSTM 1,000	**0.029**	**0.018**	**0.218**	**0.504**	**0.504**	**56**
	CNN–LSTM 1,500	0.031	0.016	0.229	0.452	0.452	84
	CNN–LSTM 2,000	0.030	0.016	0.219	0.500	0.500	134
NO_2^-–N	CNN 1,000	0.042	0.025	0.211	0.368	0.368	69
	CNN 1,500	0.041	0.023	0.206	0.394	0.394	76
	CNN 2,000	**0.039**	**0.021**	**0.195**	**0.451**	**0.451**	**120**
	CNN 2,500	0.043	0.020	0.213	0.349	0.349	130
	CNN 3,000	0.043	0.020	0.216	0.324	0.324	143
	LSTM 1,000	0.060	0.040	0.284	-0.140	-0.140	99
	LSTM 1,500	0.060	0.040	0.306	-0.324	-0.324	149
	LSTM 2,000	0.070	0.040	0.340	-0.664	-0.664	177
	LSTM 2,500	0.066	0.040	0.334	-0.612	-0.612	201
	LSTM 3,000	0.050	0.030	0.256	0.052	0.052	237
	LSTM 3,500	0.054	0.032	0.266	-0.024	-0.024	266
	LSTM 4,000	**0.046**	**0.028**	**0.246**	**0.140**	**0.140**	**322**
	LSTM 4,500	0.050	0.030	0.252	0.072	0.072	329
	LSTM 5,000	0.050	0.028	0.260	0.030	0.030	379
	CNN–LSTM 1,000	0.037	0.021	0.185	0.502	0.502	87
	CNN–LSTM 1,500	0.031	0.018	0.155	0.640	0.640	145
	CNN–LSTM 2,000	**0.028**	**0.016**	**0.141**	**0.692**	**0.696**	**188**
	CNN–LSTM 2,500	0.031	0.016	0.156	0.630	0.630	208
	CNN–LSTM 3,000	0.068	0.023	0.342	-1.467	-1.467	250
ALK	CNN 1,000	8.416	6.791	0.255	0.259	0.259	43
	CNN 1,500	8.366	6.605	0.254	0.270	0.270	78
	CNN 2,000	**7.851**	**6.292**	**0.238**	**0.357**	**0.357**	**95**
	CNN 2,500	7.970	6.392	0.242	0.338	0.338	143
	CNN 3,000	8.219	6.491	0.249	0.295	0.295	149
	LSTM 1,000	10.084	8.788	0.304	-0.060	-0.060	81
	LSTM 1,500	9.990	8.713	0.303	-0.040	-0.040	141
	LSTM 2,000	9.386	7.952	0.284	0.076	0.076	173
	LSTM 2,500	9.674	8.184	0.292	0.018	0.018	221
	LSTM 3,000	8.852	7.076	0.266	0.166	0.166	264
	LSTM 3,500	**7.914**	**6.266**	**0.238**	**0.346**	**0.346**	**275**
	LSTM 4,000	8.506	6.528	0.260	0.240	0.240	313
	LSTM 4,500	8.330	6.553	0.253	0.277	0.277	390
	CNN–LSTM 1,000	9.820	8.617	0.298	-0.005	-0.005	88
	CNN–LSTM 1,500	9.877	8.564	0.299	-0.017	-0.017	143
	CNN–LSTM 2,000	**7.766**	**6.353**	**0.235**	**0.371**	**0.371**	**189**
	CNN–LSTM 2,500	8.083	6.393	0.245	0.319	0.319	198
	CNN–LSTM 3,000	8.443	6.553	0.256	0.255	0.255	269

DO = dissolved oxygen; TAN = total ammonia nitrogen; NO_2^-–N = nitrite–nitrogen; ALK = alkalinity; RMSE = root mean square error; MAE = mean absolute error; NRMSE = normalized root mean square error; NSE = Nash–Sutcliffe efficiency; R^2 = coefficient of determination

For TAN, CNN produced the best prediction result (least error) at 1,500 epochs, LSTM at 2,000 epochs and CNN–LSTM at 1,000 epochs, with mean RMSE values of 0.027, 0.030 and 0.029, respectively. There were no significant differences for the three models between the mean prediction performance and the actual measured value. The CNN–LSTM model at 1,000 epochs had the significantly ($p < 0.01$) fastest processing time (56 s), followed by the CNN model at 1,500 epochs (83 s) and the LSTM model at 2,000 epochs (187 s), respectively.

The best epochs using CNN, LSTM and CNN–LSTM for NO_2^-–N prediction were 2,000, 4,000 and 2,000, with mean RMSE values of 0.039, 0.046 and 0.028, respectively. There were no significant differences for the models between the mean prediction performance and the actual measurements. The fastest processing time was for the CNN model at 2,000 epochs (120 s), which was significantly ($p < 0.01$) faster than the other models, followed by the CNN–LSTM model at 2,000 epochs (188 s) and the LSTM model at 4,000 epochs (322 s).

The CNN model provided the best prediction results (least error) for ALK at 2,000 epochs, the LSTM model at 3,500 epochs and the CNN–LSTM model at 2,000 epochs, with mean RMSE values of 7.851, 7.914 and 7.766, respectively. There were no significant differences for the models between the mean prediction performance and the actual measurements. However, the CNN model at 2,000 epochs had the fastest processing time (95 s), which was highly significant ($p < 0.01$) compared to the other models. This was followed by the CNN–LSTM model at 2,000 epochs (189 s) and the LSTM model at 3,500 epochs (275 s).

The mean values for RMSE, MAE, NRMSE, NSE, R^2 and processing time for all models are presented in Table 2 and Fig. 4. The comparison of prediction efficiency with actual measurements is shown in Figs. 5A–5D.

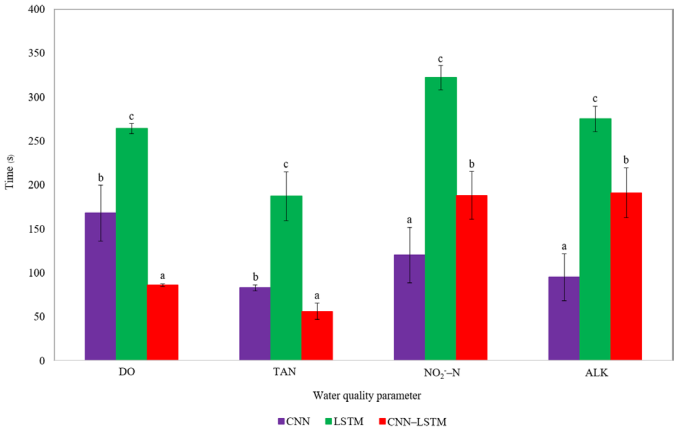

Fig. 4 Mean processing times for three different models (convolutional neural network (CNN), long short–term memory (LSTM) and a hybrid CNN–LSTM model) across 4 predicted water quality parameters—dissolved oxygen (DO), total ammonia nitrogen (TAN), nitrite-nitrogen (NO_2^-–N) and alkalinity (ALK). Different lowercase letters above columns indicate highly significant ($p < 0.01$) differences between models within each parameter

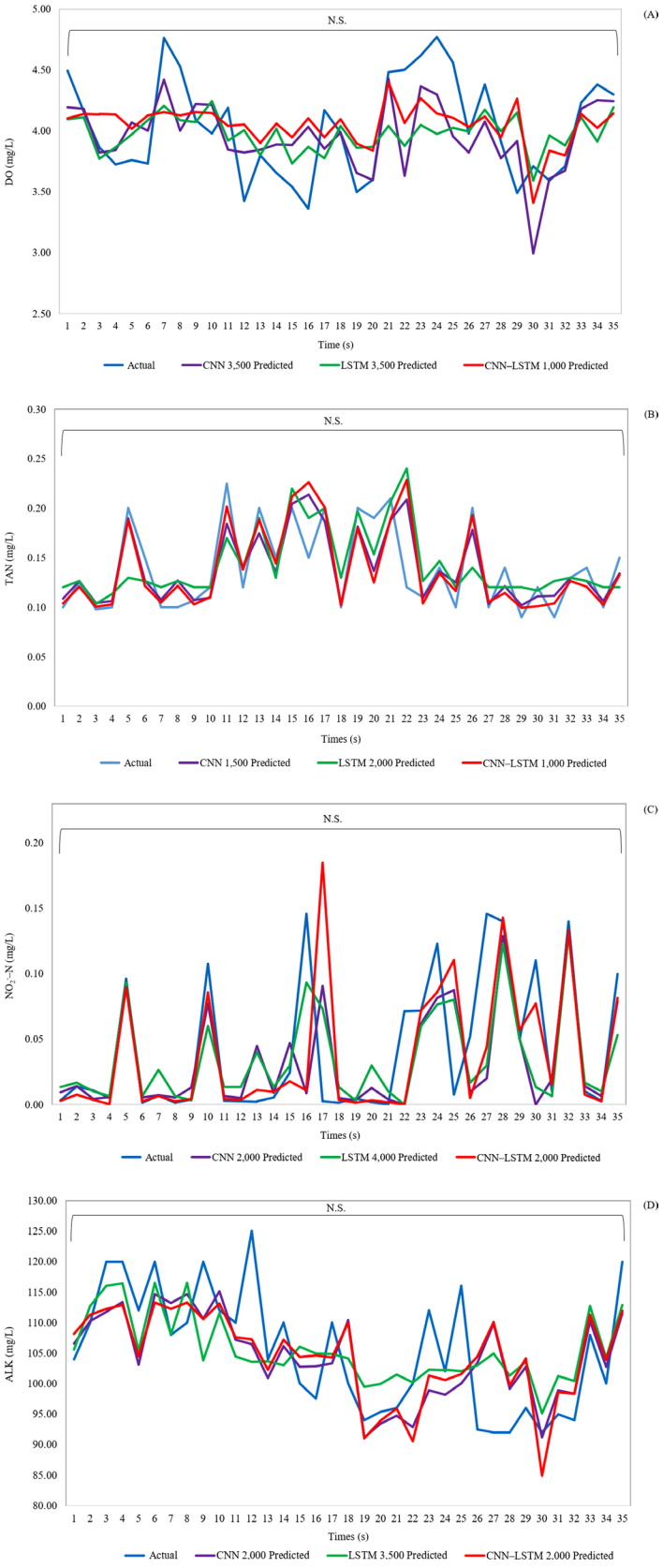

Fig. 5 Prediction of important water quality values using three optimized models [convolutional neural network (CNN), long short–term memory (LSTM) and a hybrid CNN–LSTM model]: (A) dissolved oxygen (DO); (B) total ammonia nitrogen (TAN); (C) nitrite-nitrogen (NO_2^-–N); (D) alkalinity (ALK). N.S. indicates no significant difference, while a significant difference

Discussion

The overall water quality parameters based on the data collection were in appropriate ranges for red tilapia culture. For example, the mean DO was more than 3 mg/L (Kolding et al., 2008; Tran-Duy et al., 2012), Temp was in the range 25–32°C (Azaza et al., 2008) and the pH was in the range 7–8 (Lawson, 1995; El-Sherif and El-Feky, 2009). Furthermore, the mean TAN was less than 0.5 mg/L (Hargreaves and Tucker, 2004) and the mean NO_2^-–N was less than 0.5 mg/L (Lawson, 1995, Stone and Thomforde, 2004), while the mean ALK was in the range 75–400 mg/L (Lawson, 1995; Boyd and Tucker, 2012) and the mean Trans was in the range 19–110 cm. None of the parameters have been reported to affect the feeding and behavior of red tilapia in river–cage farming (Taparhudee et al., 2024).

Based on the current results, the hybrid model (CNN–LSTM) had superior performance in predicting all parameters. The hybrid model could effectively capture the spatial and temporal relationships, resulting in higher prediction accuracy compared to using only the CNN or LSTM models. Furthermore, the CNN–LSTM hybrid model showed advantages in performance, with shorter computation times due to fewer epochs being required for optimality, making it a suitable choice for covariate water quality prediction in this study. The results of this study were consistent with Baek et al. (2020), who applied a similar model to capture the temporal variations of pollutants in the Nakdong River Basin. Li et al. (2022) concluded that the hybrid model was effective for estimating water availability and managing flood alerts. Li et al. (2023) introduced an attention–based CNN–LSTM model for effluent wastewater quality prediction. Pan et al. (2023) developed a CNN–LSTM algorithm to estimate particulate organic carbon concentration in lakes using Sentinel 2 satellite images and water surface sample data. Jongjaraunsuk et al. (2024) compared the performance of DL models and a hybrid model for predicting key water quality parameters in an outdoor RAS for red tilapia, finding that the CNN–LSTM produced the best results.

However, the performance parameters for ALK prediction were higher than for the other predicted water quality parameters, perhaps because the ALK dataset covered a wider range or there was greater variability compared to DO, TAN and NO_2^-–N . Hence, the model might be challenged if used to make more accurate predictions, as higher variability generally increases prediction error metrics (Kuhn and Johnson, 2013).

Some limitations of this study were that the model was trained and tested on a specific dataset related to the red tilapia river–based culture system. Therefore, generalization of the results may not be appropriate to other aquaculture systems or different species of fish. Furthermore, the study did not account for extreme or unusual environmental conditions that might affect water quality parameters and model performance. such as sudden changes in weather, pollution events or unexpected biological activity, that could influence the accuracy of predictions.

Future studies should explore methods to enhance the time efficiency and predictive accuracy of the CNN–LSTM model, such as incorporating adaptive learning rates, hybrid techniques with other models or advanced validation strategies, such as K–fold cross–validation, particularly with temporal adaptations (rolling–window splits) to address time–series dependencies. This would provide additional model robustness across diverse data distributions and optimize hyperparameters for real–world deployment. Additionally, extending the framework to other aquaculture systems could confirm its broader applicability and effectiveness under varying environmental conditions. The CNN–LSTM model's superior accuracy over standalone CNN or LSTM architectures, combined with its adaptability to dynamic water quality changes, positions it as a promising tool for real–time monitoring. Further development could focus on lightweight implementations for edge devices, enabling scalable, low–latency decision–making in commercial aquaculture operations.

Conclusion

The current study aimed to enhance the efficiency and effectiveness of water quality monitoring in red tilapia river-based aquaculture systems by developing a predictive model using easily measurable water quality parameters (Temp, pH and Trans) to predict important but difficult to measure water quality parameters (DO, TAN, NO_2^-–N and ALK). Three DL model (CNN, LSTM and a hybrid CNN–LSTM) were tested by tuning the epochs, starting with 1,000 and gradually increased the count by 500 in each step. This process continued until there was a decrease in accuracy (notably in the high–performance metrics: RMSE, MAE, NRMSE, NSE and R^2). Based on the results, the hybrid model based on CNN–LSTM had superior performance in predicting all parameters. The hybrid model could effectively capture the spatial and temporal relationships, resulting in higher prediction accuracy compared to using only

the CNN or LSTM models. Furthermore, the CNN–LSTM hybrid model had better performance, with shorter computation times due to fewer epochs being needed to reach optimality. Future studies should focus on enhancing the CNN–LSTM model's time efficiency and accuracy through adaptive learning rates or hybrid techniques and should explore its applicability across various aquaculture systems for real–time water quality management.

Conflict of interest

The authors declare that there are no conflicts of interest.

Acknowledgements

This study was funded by the Faculty of Fisheries, Kasetsart University, Bangkok, Thailand under the project "Optimal approach for predicting water quality in red tilapia river-based cage culture based on machine learning". The research facilities were made available by the staff in the Aquacultural Engineering Laboratory, Kasetsart University and Fishbear Farm, Kanchanaburi, Thailand.

References

Ahmed, U., Mumtaz, R., Anwar, H., Shah, A.A., Irfan, R., García-Nieto, J. 2019. Efficient water quality prediction using supervised machine learning. Water. 11: 2210. doi.org/10.3390/w11112210

Alzubaidi, L., Zhang, J., Humaidi, A.J., et al. 2021. Review of deep learning: concepts, CNN architectures, challenges, applications, future directions. J. Big Data. 8: 53. doi.org/10.1186/s40537-021-00444-8

Anand, M.V., Sohitha, C., Saraswathi, G.N., Lavanya, G.V. 2023. Water quality prediction using CNN. J. Phys. Conf. Ser. 2428: 012051. doi.org/ 10.1088/1742-6596/2484/1/012051

American Public Health Association, American Water Work Association, Water Pollution Control Federation. 2005. Standard Methods of the Examination of Water and Wastewater. American Public Health Association. Washington DC, USA

Azaza, M.S., Dhraïef, M.N., Kraïem, M.M. 2008. Effects of water temperature on growth and sex ratio of juvenile Nile tilapia *Oreochromis niloticus (*Linnaeus*)* reared in geothermal waters in southern Tunisia. J. Therm. Biol. 33: 98–105. doi.org/10.1016/ j.jtherbio.2007.05.007

Baek, S.-S., Pyo, J., Chun, J.A. 2020. Prediction of water level and water quality using a CNN-LSTM combined deep learning approach. Water. 12(12), 3399. doi.org/10.3390/w14091322

Boyd, C.E. 1982. Water Quality Management for Pond Fish Culture. Elsevier Scientific Publishing Company. Amsterdam, the Netherlands.

Boyd, C.E., Tucker, C.S. 2012. Pond Aquaculture Water Quality Management. Springer Science & Business. New York, NY, USA.

Cai, H., Zhang, C., Xu, J., Wang, F., Xiao, L., Huang, S., Zhang, Y. 2023. Water quality prediction based on the KF-LSTM encoder-decoder network: a case study with missing data collection. Water. 15: 2542. doi.org/10.3390/w15142542

Castrillo, M., López García, A. 2020. Estimation of high frequency nutrient concentrations from water quality surrogates using machine learning methods. Water Res. 172: 115490. doi.org/10.1016/j.watres.2020.115490

Chen, F., Du, Y., Qiu, T., et al. 2021. Design of an intelligent variable-flow recirculating aquaculture system based on machine learning methods. Appl. Sci. 11: 6545. doi.org/10.3390/app11146546

Chen, H., Yang, J., Fu, X., et al. 2022. Water quality prediction based on LSTM and attention mechanism: a case study of the Burnett River, Australia. Sustainability. 14: 13231. doi.org/10.3390/su142013231

El-Sherif, M.S., El-Feky, A.M.I. 2009. Performance of Nile tilapia (*Oreochromis niloticus*) fingerlings. I. Effect of pH. Int J Agric Biol. 11: 297–300.

Food and Agricultural Organization of the United Nations. 2022. The state of world fisheries and aquaculture. https://www.fao.org/3/cc0461en/cc0461en.pdf, 9 May 2024.

Ganesh, K., Carole, R.E. 2016. Technological advances that led to growth of shrimp, salmon and tilapia farming. Rev. Fish. Sci. Aquac. 24: 136–152. doi.org/10.1080/23308249.2015.1112357

Hargreaves, J.A., Tucker, C.S. 2004. Managing Ammonia in Fish Ponds. Southern Regional Aquaculture Center. Stoneville, NC, USA.

Jiang, C., Chen, Y., Chen, S., Bo, Y., Li, W., Tian, W., Guo, J. 2019. A mixed deep recurrent neural network for MEMS gyroscope noise suppressing. Electronics. 8: 181. doi.org/10.3390/electronics8020181

Jongjaraunsuk, R., Taparhudee, W., Suwannasing, P. 2024. Comparison of water quality prediction for red tilapia aquaculture in an outdoor recirculation system using deep learning and a hybrid model. Water. 16: 907. doi.org/10.3390/w16060907

Juna, A., Umer, M., Sadiq, S., Karamti, H., Eshmawi, A.A., Mohamed, A., Ashraf, I. 2022. Water quality prediction using KNN imputer and multilayer perceptron. Water. 14: 2592. doi.org/ 10.3390/w14172592

Kolding, J., Haug, L., Stefansson, S. 2008. Effect of ambient oxygen on growth and reproduction in Nile tilapia (*Oreochromis niloticus*). Can. J. Fish. Aquat. Sci. 65: 1413–1424. doi.org/10.1139/F08-059

Kuhn, M., Johnson, K. 2013. Applied Predictive Modeling. Springer Science & Business. New York, NY, USA.

Lawson, T.B. 1995. Fundamental of Aquaculture Engineering. Chapman and Hall. New York, NY, USA.

Li, T., Lu, J., Wu, J., Zhang, Z., Chen, L. 2022. Predicting aquaculture water quality using machine learning approaches. Water. 14: 2836. doi.org/ 10.3390/w14182836

Li, Y., Kong, B., Yu, W., Zhu, X. 2023. An attention-based CNN-LSTM method for effluent wastewater quality prediction. Appl. Sci. 13: 7011. doi.org/10.3390/app13127011

Lin, Y., Yan, Y., Xu, J., Liao, Y., Ma, F. 2021. Forecasting stock index price using the CEEMDAN-LSTM model. N. Am. J. Econ. Finance. 57: 101421. doi.org/10.1016/j.najef.2021.101421

Liu, P., Wang, J., Sangaiah, A.K., Xie, Y., Yin, X. 2019. Analysis and prediction of water quality using LSTM deep neural networks in IoT environment. Sustainability. 11: 2058. doi.org/10.3390/su11072058

Palani, S., Liong, S.Y., Tkalich, P. 2008. An ANN application for water quality forecasting. Mar. Pollut. Bull. 56: 1586–1597. doi.org/10.1016/j.marpolbul.2008.05.021

Pan, B., Yu, H., Cheng, H., Du, S., Cai, S., Zhao, M., Du, J., Xie, F. 2023. ACNN–LSTM machine-learning method for estimating particulate organic carbon from remote sensing in lakes. Sustainability. 15: 13043. doi.org/10.3390/ su151713043

Stone, N.M, Thomforde, H.K. 2004. Understanding your fish pond water analysis report. https://fisheries.tamu.edu/files/2013/09/Understanding-Your-Fish-Pond-Water-Analysis-Report.pdf, 12 May 2024.

Taparhudee, W., Jongjaraunsuk, R., Nimitkul, S., Suwannasing, P., Mathurossuwan, W. 2024. Application of unmanned aerial vehicle with computer vision as a tool for welfare monitoring of cage-cultured, river-based hybrid red tilapia. Agr. Nat. Resour. 58, 313–320. doi.org/10.34044/j.anres.2024.58.3.04

Tran-Duy, A., van Dam, A.A., Schrama, J.W. 2012. Feed intake, growth and metabolism of Nile tilapia (*Oreochromis niloticus*) in relation to dissolved oxygen concentration. Aquac. Res. 43: 730–744. doi.org/10.1111/j.1365-2109.2011.02882.x

Wang, X., Li, Y., Qiao, Q., Tavares, A., Liang, Y. 2023. Water quality prediction based on machine learning and comprehensive weighting methods. Entropy. 25: 1186. doi.org/10.3390/e25081186

Wu, J., Wang, Z. 2022. A hybrid model for water quality prediction based on an artificial neural network, wavelet transform and long short-term memory. Water. 14: 610. doi.org/ 10.3390/w14040610

Yang, J., Jia, L., Guo, Z., Shen, Y., Li, X., Mou, Z., Yu, K., Lin, J.C.W. 2023. Prediction and control of water quality in Recirculating Aquaculture System based on hybrid neural network. Eng. Appl. Artif. Intell. 121: 106002. doi.org/10.1016/j.engappai.2023.106002

Ye, B., Cao, X., Liu, H., Wang, Y., Tang, B., Chen, C., Chen, Q. 2022. Water chemical oxygen demand prediction model based on the CNN and ultraviolet-visible spectroscopy. Front. Environ. Sci. 10: 1027693. doi.org/ 10.3389/fenvs.2022.1027693

You, W., Shen, C., Wang, D., Chen, L., Jiang, X., Zhu, Z. 2020. An intelligent deep feature learning method with improved activation functions for machine fault diagnosis. IEEE access. 8: 1975–1985. doi.org/10.1186/s40537-021-00444-8

Zambrano, A.F., Giraldo, L.F., Quimbayo, J., Medina, B., Castillo, E. 2021. Machine learning for manually-measured water quality prediction in fish farming. PLOS One. 16: e0256380. doi.org/10.1371/journal.pone.0256380

Zhou, S., Song, C., Zhang, J., Chang, W., Hou, W., Yang, L. 2022. A hybrid prediction framework for water quality with integrated W-ARIMA-GRU and LightGBM methods. Water. 14: 1322. doi.org/10.3390/w14091322